

Synthesis and stereodynamics of intramolecular hemiacetals in biaryl aldehyde-alcohols

Simone Heitsch | Lena Carina Mayer | Yanis Luca Pignot  | Oliver Trapp 

Department of Chemistry, Ludwig-Maximilians-University Munich, Munich, Germany

Correspondence

Oliver Trapp, Department of Chemistry, Ludwig-Maximilians-University Munich, Butenandtstrasse 5-13, 81377 Munich, Germany.

Email: oliver.trapp@cup.uni-muenchen.de

Funding information

European Research Council (ERC), Grant/Award Number: 258740

Abstract

Soai's asymmetric autocatalysis represents a highly remarkable example for spontaneous symmetry breaking and enantioselective amplification in the enantioselective alkylation of pyrimidine-5-carbaldehydes to the corresponding chiral pyrimidine alcohols. Recently, zinc hemiacetalate complexes, formed from pyrimidine-5-carbaldehydes and the chiral product alcohol, were identified by in situ high-resolution mass spectrometric measurements as highly active transient asymmetric catalysts in this autocatalytic transformation. To study the formation of such hemiacetals and their stereodynamic properties, we focused on the synthesis of coumarin homolog biaryl systems with carbaldehyde and alcohol substituents. Such systems are able to form hemiacetals by intramolecular cyclization. An interesting feature of the substituted biaryl backbone is that *tropos* and *atropos* systems can be obtained, enabling or disabling the intramolecular cyclization to hemiacetals. Biaryl structures with various functional groups were synthesized, and the equilibrium and stereodynamics between the closed and open structures were investigated by dynamic enantioselective HPLC (DHPLC). The enantiomerization barriers ΔG^\ddagger and activation parameters ΔH^\ddagger and ΔS^\ddagger were determined from temperature dependent kinetic measurements.

KEYWORDS

atropisomer, biphenyl, chiral HPLC, coumarin, enantiomerization, enantioselective dynamic HPLC, hemiacetal, interconversion, intramolecular cyclization, phenylpyridine

1 | INTRODUCTION

The selective formation of enantiomerically pure compounds plays a significant role for biomolecules in nature. Homochirality of biomolecular building blocks is mandatory for the reproducible replication as well as in

recognition processes and therefore for the evolution of life.^{1,2} The study of asymmetric catalysis and autocatalysis are of great interest because of potential non-linear effects and amplification of enantiomeric excesses (*ee*'s).^{3,4} Such systems can provide hints to the development of homochirality in nature. In particular, systems

[This article is part of the Special issue: Proceedings from 32nd International Symposium on Chirality, 2022 Chicago, US. See the first articles for this special issue previously published in Volume 35:8. More special articles will be found in this issue as well as in those to come.]

This is an open access article under the terms of the [Creative Commons Attribution-NonCommercial](https://creativecommons.org/licenses/by-nc/4.0/) License, which permits use, distribution and reproduction in any medium, provided the original work is properly cited and is not used for commercial purposes.

© 2023 The Authors. *Chirality* published by Wiley Periodicals LLC.

yielding high *ee*'s starting from very low *ee*'s are the most interesting.⁵ Soai's asymmetric autocatalysis fulfills all these criteria. In an asymmetric autocatalytic reaction, the chiral reaction product serves as a catalyst, selectively catalyzing its own formation.⁶ In 1990, Soai et al. realized this in the addition of Zn (*i*Pr)₂ to pyridine-3-carbaldehyde⁷ and later to pyrimidine-5-carbaldehydes showing pronounced autocatalytic properties.⁸ Several research groups have been engaged in the mechanistic investigation of this fascinating reaction. Besides Soai and co-workers,^{9–11} the groups of Blackmond,¹² Brown et al.,^{13,14} and Amedjkouh et al.^{15–17} focused on the elucidation of the Soai reaction by experimental investigations.¹⁸ Recent mechanistic investigations by the groups of Denmark^{19,20} and Trapp^{21,22} proposed two different mechanistic approaches.²³ In 2020, Denmark et al. proposed a homo-chiral tetramer in a square-macrocycle-square conformation of the product alkoxide as catalytically active species in the Soai reaction.^{21,22} Trapp et al. proposed a different mechanism for the Soai reaction, based on identified hemiacetalate complexes, which are formed from the aldehyde and Zn-alkoxide. The configuration of the Zn-alkoxides determines the configuration of the newly formed stereogenic center of the hemiacetalate.²³ The identified transient Zn-hemiacetalate-catalyst has *R,R* or *S,S* configuration (cf. Figure 1), which is highly efficient in coordinating the substrate and Zn (*i*Pr)₂ leading to an enantioselective alkylation and propagation of the *R* or *S* configuration, respectively. The formation of the transient hemiacetalate catalyst has a barrier ΔG^\ddagger of 82.6 kJ/mol,²³ which also explains the long induction period. Doping experiments by transferring the formed transient hemiacetalate catalyst at the apex of formation from a reacting Soai reaction to a freshly prepared reaction mixture shift the inflection point of the *s*-shaped reaction profile (cf. Figure 2A, solid line), thereby shortening the induction period by 55 sec compared to the normal

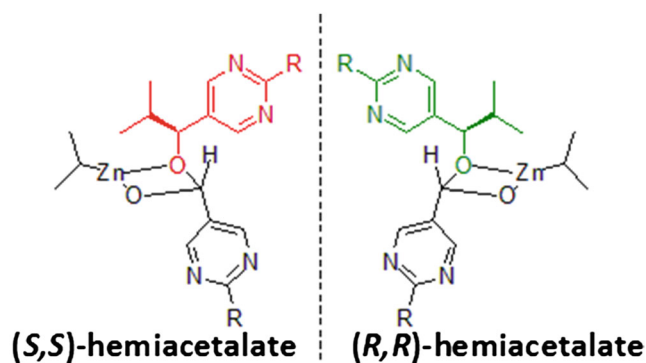


FIGURE 1 Identified catalytically active transient Zn-hemiacetalate-complex explaining the autocatalytic behavior of the Soai's asymmetric autocatalysis.²³

reference reaction (cf. Figure 2A, dashed line). Such a significant shift is not observed when a Soai reaction is doped with the same amount of a completed reaction or addition of the product Zn-alkoholate, proving that the alcohol itself is not the catalyst.²³

Therefore, we focus on the stereodynamics of coumarin homolog biaryl structures, which are able to form intramolecular hemiacetals (cf. Figure 2B).

These structures are interesting from two perspectives: Such systems can form *tropos* biaryls with high stereodynamic flexibility or can be atropisomers, if the free rotation around the central σ -bond is hindered by substituents,^{25–30} naphthyl moieties or bridging cyclic structures.³¹ Furthermore, the combination of the carbaldehyde and alcohol moiety enable an equilibrium

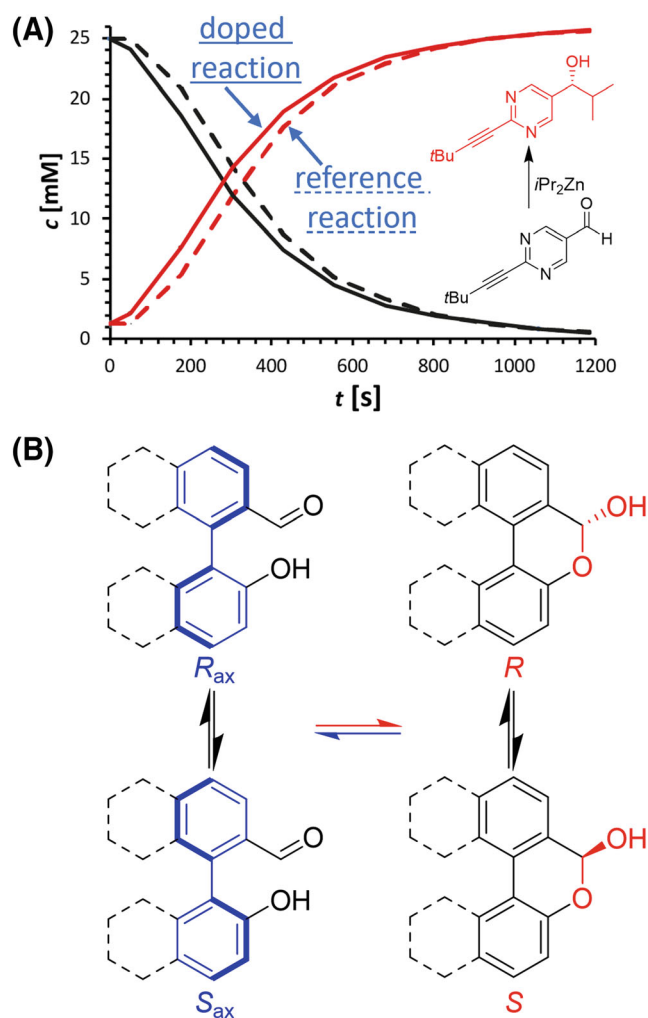


FIGURE 2 (A) Reaction progress of the autocatalytic conversion of (2-(tert-butylacetylene-1-yl)pyrimidine-5-carbaldehyde (black) and (*R*)-2-(tert-butylacetylene-1-yl)pyrimidine-5-(iso-butan-1-ol) (red) in Soai's reaction. With (solid line) and without (dashed line) initial presence of the transient catalyst. (B) Dynamic structure motif forming hemiacetals.²⁴

between the open form and a six-membered ring. Upon ring-closure, a stereogenic center is formed by the hemiacetal, while the stereogenic axis is getting simultaneously lost by planarization of the system. In addition, it represents potentially another interesting example for Mislow's paradox, where an interconversion between enantiomers becomes possible along a chirality-preserving path.^{32,33}

In context of Soai's asymmetric autocatalysis, such hemiacetals can serve as substrate and catalyst-ligand at the same time. In general, such motifs are of interest to design and synthesize self-adaptable catalysts.³⁴⁻³⁷ However, it is important to note that the hemiacetals in Soai's asymmetric autocatalysis are formed by intermolecular reaction of the formed alcohol with the substrate aldehyde, whereas the presented hemiacetals here are obtained by an intramolecular reaction.

Here, we synthesized eight structures that contain a combination of such stereodynamic motifs, which are also found in natural products, as exemplified in substituted 1-(2'-hydroxyphenyl)-naphthalene-2-carbaldehydes and their equilibria between open hydroxy aldehydes and cyclic lactol structures.³⁸ We studied this structural motif with respect to a potential directional shift of the equilibrium depending on the aryl residues of the biaryl moiety. The stereodynamic behavior and the ring closing properties of the prepared structures were analyzed by enantioselective dynamic HPLC (DHPLC)³⁹⁻⁴³ experiments and solvent dependent NMR measurements.

2 | MATERIALS AND METHODS

2.1 | General procedures

All air and moisture sensitive reactions were carried out under Ar atmosphere, which has been dried over silica gel and molecular sieve (4 Å). Standard Schlenk technique was applied and all glassware was flame-dried before use.

2.2 | Solvents and reagents

Anhydrous solvents were used as received from Sigma-Aldrich Chemie GmbH stored under dry argon and molecular sieve (3 Å) or were taped from the solvent purification system MBraun SPS-800 and used immediately. Degassed solvents were prepared according to the pump-thaw process in three successive freezing cycles and subsequently stored under Ar in Young ampoules. All chemicals were purchased from manufacturing and

trading companies (abcr GmbH, Sigma-Aldrich-Merck) used without further purification.

2.3 | Analytical methods

NMR spectra were recorded on a Bruker Avance III HD spectrometer (400 MHz). The multiplicity is abbreviated as the following: s (singlet), d (doublet), t (triplet), and m (multiplet). Multiple coupling signals were assigned using subscripted abbreviations as described. The atom numbering is not based on IUPAC nomenclature. The assignment was performed by two-dimensional experiments (¹H-¹H-COSY, ¹H-¹³C-HSQC, and ¹H-¹³C-HMBC). Mass spectroscopic data was collected with a Thermo Q Exactive Plus Hybrid Quadrupole Orbitrap mass spectrometer using electrospray ionization (ESI). For solid-state IR analysis, a Thermo Fisher Nicolet 6700 FT-IR-Spectrometer was used. Column chromatography was performed using silica gel (pore size 60 Å, 70–230 mesh, 63–200 μm) obtained from Sigma-Aldrich Chemie GmbH. Thin layer chromatography was performed on coated aluminum sheets (Machery-Nagel POLYGRAM SILG/UV 254). Components were visualized by fluorescence through irradiation with UV light (254 nm). HPLC-MS measurements were carried out on an Agilent Technologies 1200 HPLC-MS (Agilent Technologies, California, USA), equipped with a binary solvent pump, membrane solvent degasser, an autosampler, DAD detector, and a quadrupole mass spectrometer Agilent 6120, equipped with an APCI source. All solvents used for HPLC-MS experiments (*n*-hexane, isopropyl alcohol) were used in HPLC-grade quality and provided by Sigma-Aldrich-Merck.

2.4 | Synthesis

2.4.1 | Procedure for optimized Suzuki-coupling A

A flame dried round bottom flask was charged with halogen aldehyde (1.00 equiv.), boronic acid (1.50 equiv.), and sodium carbonate (2.30 equiv.). The educts were dissolved in degassed THF, MeOH, and water. Afterwards, bis (triphenyl-phosphine)palladium (II) dichloride (0.11 equiv.) was added, and the mixture was refluxed over night at 70°C. Subsequently, the reaction mixture was diluted with water and EtOAc (1:2). The layers were separated and extracted three times with EtOAc. The combined organic layers were dried over Na₂SO₄. The solvent was removed in vacuo, and the crude product was purified via column chromatography.

2.4.2 | Procedure for optimized Suzuki-coupling **B**

A flame dried round bottom flask was charged with halogen aldehyde (1.00 equiv.), boronic acid (1.36 equiv.), and sodium carbonate (3.90 equiv.). The educts were dissolved in DME, EtOH, and/or degassed water. The mixed solution was subsequently degassed by passing argon through a cannula for 1 h. Afterwards, tetrakis (triphenyl-phosphine)palladium(0) (0.10 equiv.) was added, and the mixture was refluxed over night at 80°C. Subsequently, the reaction mixture was diluted with water. The layers were separated and extracted three times with diethyl ether. The combined organic layers were dried over Na₂SO₄. The solvent was removed in vacuo, and the crude product was purified via column chromatography.

2.4.3 | 2'-Hydroxy-[1,1'-binaphthalene]-2-carbaldehyde (**3**)

Compound **3** was prepared according to literature.⁴⁴ A flame dried round bottom flask was charged with binaphto[2,1-b:1',2'-d]furan **2**¹¹ (1.40 g, 5.22 mmol, 1.00 equiv.) and dissolved in anhydrous diethyl ether (50 ml) and toluene (16 ml) under argon atmosphere. Lithium (79.7 mg, 11.5 mmol, 2.20 equiv.) was added at 0°C, and the reaction mixture was stirred for 24 h at room temperature. The reaction mixture was cooled to -78°C, and DMF (323 µl, 4.17 mmol, 0.80 equiv.) was added. The suspension was stirred for 2 h at the set temperature and then for additional 15 h at room temperature. The reaction was quenched with hydrochloric acid (3 M, 30 ml). Subsequently, the organic layer was separated, washed with hydrochloric acid (3-30 ml), and dried over Na₂SO₄. The solvent was removed in vacuo, and the crude product was purified via column chromatography (silica, *n*-pentane:EtOAc, 5:1, R_f = 0.219). 2'-Hydroxy-[1,1'-binaphthalene]-2-carbaldehyde **3** (0.797 g, 2.67 mmol, 51%) was obtained as a light brown solid.

¹H NMR (600 MHz, CDCl₃, T = 293.15 K, δ): 9.70 (s, 1H), 8.21 (d, ³J = 8.6 Hz, 1H), 8.11 (d, ³J = 8.7 Hz, 1H), 8.01 (d, ²J = 8.3 Hz, 1H), 7.99 (d, ²J = 8.9 Hz, 1H), 7.90 (d, ²J = 8.2 Hz, 1H), 7.66 (d_d, ^{2,2}J = 8.2, 6.7 Hz, 1H), 7.46 (d_d, ²J = 8.5, ³J = 1.2 Hz, 1H), 7.40 (d_d, ²J = 8.4, ³J = 1.2 Hz, 1H), 7.38-7.35 (m, 1H), 7.34 (d, ²J = 9.0 Hz, 1H), 7.26 (m, 1H), 6.95 (d, ²J = 8.6 Hz, 1H), 4.75 (s, 1H).

¹³C NMR (151 MHz, CDCl₃, T = 293.15 K): δ (ppm) = 192.1, 151.6, 138.5, 136.7, 134.4, 133.3, 132.5, 131.0, 129.8, 129.5, 128.8, 128.6, 128.1, 127.7, 127.4, 126.7, 124.6, 123.9, 122.6, 117.4, 113.6.

HR-MS (EI⁺, chloroform): [M + H]⁺: C₂₁H₁₄O₂ + H⁺, calculated m/z 299.1067, found m/z 299.1030.

IR (KBr): ν = 3376.1, 1680.1, 1664.3, 1616.8, 1593.7, 1514.2, 1428.9, 1380.1, 1273.6, 1231.0, 1201.1, 1172.9, 1142.9, 975.3, 871.3, 819.6, 690.3, 669.6 cm⁻¹.

2.4.4 | 1-(2-Chloro-6-hydroxyphenyl)-2-naphthaldehyde (**7**)

1-Bromo-2-naphthaldehyde⁴⁵ (1.00 g, 4.25 mmol, 1.00 equiv.), (2-chloro-6-hydroxyphenyl)boronic acid (1.03 g, 5.80 mmol, 1.36 equiv.), and sodium carbonate (1.76 g, 16.6 mmol, 3.9 equiv.) were added to a flame dried round bottom flask and dissolved in DME (120 ml) and degassed water (30 ml). Tetrakis (triphenylphosphine) palladium(0) was added (12.3 mg, 10.6 µmol, 0.05 equiv.), and the suspension was refluxed for 24 h at 80°C. Water (50 ml) was added, the layers were separated, and the aqueous layer was extracted with diethyl ether (3-50 ml). The crude product was purified via column chromatography (silica, *n*-pentane:EtOAc, 10:1 to 3:1, R_f[3:1] = 0.564). 1-(2-Chloro-6-hydroxyphenyl)-2-naphthaldehyde **7** (978 mg, 3.46 mmol, 81%) was obtained as a yellow solid.

¹H NMR (600 MHz, CDCl₃, T = 293.15 K, δ): 9.89 (s, 1H), 8.13 (d, ²J = 8.6 Hz, 1H), 8.05 (d, ²J = 8.6 Hz, 1H), 7.98 (d, ²J = 8.1 Hz, 1H, H3), 7.71-7.65 (m, 1H), 7.57-7.51 (m, 2H), 7.40 (t, ²J = 8.2 Hz, 1H), 7.21 (d_d, ²J = 8.2 Hz, ³J = 1.0 Hz, 1H), 7.02 (d, ²J = 8.3 Hz, 1H), 4.75 (s, 1H).

¹³C NMR (151 MHz, CDCl₃, T = 293.15 K, δ): 191.52, 154.84, 137.41, 136.48, 135.23, 132.19, 131.54, 130.85, 129.94, 129.39, 128.64, 127.80, 125.98, 122.50, 121.90, 120.74, 114.31.

HR-MS (ESI⁺, EtOAc): [M-H]⁻: C₁₇H₁₁O₂Cl-H⁻, calculated m/z 281.0375, found m/z 281.0375.

IR (KBr): ν = 3148.8, 1687.8, 1660.5, 1617.8, 1594.5, 1444.9, 1329.7, 1287.3, 1243.5, 1028.8, 975.7, 900.5, 819.0, 782.1, 670.5 cm⁻¹.

2.4.5 | 6H-Naphtho[2,1-c]chromen-6-ol (**8**)

The reaction followed synthesis procedure **A**. 1-Bromo-2-naphthaldehyde^{44,45} (1.00 g, 4.25 mmol), (2-hydroxyphenyl)boronic acid (880 mg, 6.38 mmol), sodium carbonate (1.04 g, 9.78 mmol), and bis (triphenylphosphine)palladium (II) dichloride (328 mg, 468 µmol) were dissolved in THF (15 ml), MeOH (10 ml), and water (7 ml). Purification via column chromatography (silica, cyclo-hexane:EtOAc; 3:1, R_f = 0.810) served 6H-naphtho [2,1-c]chromen-6-ol **8** (568 mg, 2.29 mmol, 54%) as a light brown solid.

^1H NMR (800 MHz, CDCl_3 , T = 293.15 K, δ): 8.63 (d, $^3J = 8.4$ Hz, 1H), 8.11 (d, $^3J = 8.3$ Hz, 1H), 7.81 (d, $^2J = 7.8$ Hz, $^3J = 1.8$ Hz, 1H), 7.67 (s, 1H), 7.55–7.45 (m, 4H), 7.26–7.22 (m, 1H), 7.02 (d, $^2J = 8.3$ Hz, 1H), 6.76 (s, 1H).

^{13}C NMR (201 MHz, CDCl_3 , T = 293.15 K, δ): 151.6, 135.0, 130.2, 129.7, 129.0, 128.9, 128.63, 128.59, 126.9, 126.5, 126.3, 125.7, 123.4, 122.9, 122.7, 118.8, 93.80.

HR-MS (ESI⁺, chloroform): $[\text{M}-\text{H}_2\text{O}]^+$: $\text{C}_{17}\text{H}_{12}\text{O}_2-\text{H}_2\text{O}^+$, calculated m/z 231.0804, found m/z 231.0807.

IR (KBr): $\nu = 3098.2, 1596.7, 1483.2, 1451.4, 1393.1, 1234.1, 1196.1, 1102.8, 1049.7, 1037.1, 996.6, 963.1, 916.0, 804.0, 782.2, 751.9, 686.0$ cm^{-1} .

2.4.6 | 5H-Chromeno[3,4-b]pyridin-5-ol (**12**)

The reaction followed synthesis procedure **B**. 3-Chloropicolin-aldehyde (500 mg, 3.53 mmol), (2-hydroxyphenyl)boronic acid (731 mg, 5.30 mmol), sodium carbonate (3.18 g, 30.0 mmol), and tetrakis (triphenylphosphine)palladium(0) (408 mg, 353 μmol) were dissolved in DME (27 ml), EtOH (14 ml), and water (10 ml). Purification via column chromatography (silica, cyclohexane:EtOAc; 1:1, $R_f = 0.405$) served 5H-chromeno[3,4-b]bipyridin-5-ol **12** (255 mg, 1.28 mmol, 36%) as a colorless solid.

^1H NMR (600 MHz, CDCl_3 , T = 293.15 K, δ): 8.57 (d, $^2J = 4.9$ Hz, $^3J = 1.5$ Hz, 1H), 8.20 (d, $^2J = 8.0$ Hz, $^3J = 1.4$ Hz, 1H), 7.80 (d, $^2J = 7.8$ Hz, $^3J = 1.5$ Hz, 1H), 7.49 (d, $^2J = 8.0$ Hz, $^3J = 4.8$ Hz, 1H), 7.38 (t, $^2J = 8.1$ Hz, $^3J = 7.3$ Hz, 1H), 7.19 (m, 1H), 7.16 (m, 1H), 6.57 (s, 1H).

^{13}C NMR (101 MHz, CDCl_3 , T = 293.15 K, δ): 150.7, 149.0, 147.6, 130.8, 130.5, 124.9, 124.8, 123.2, 122.6, 118.8, 92.1.

HR-MS (ESI⁺, EtOAc): $[\text{M} + \text{H}]^+$: $\text{C}_{12}\text{H}_9\text{NO}_2 + \text{H}^+$, calculated m/z 200.0706, found m/z 200.0707.

IR (KBr): $\nu = 2704.6, 1608.5, 1571.7, 1454.8, 1418.1, 1302.3, 1248.4, 1206.2, 1195.8, 1107.9, 1054.0, 1042.0, 995.6, 885.6, 851.2, 819.5, 780.8, 738.5, 699.3$ cm^{-1} .

2.4.7 | 5H-Chromeno[4,3-b]pyridin-5-ol (**11**)

The reaction followed synthesis procedure **B**. 2-Chloronicotin-aldehyde (500 mg, 3.53 mmol), (2-hydroxyphenyl)boronic acid (731 mg, 5.30 mmol), sodium carbonate (3.18 g, 30.0 mmol), and tetrakis (triphenylphosphine)palladium(0) (408 mg, 353 μmol) were dissolved in DME (27 ml), EtOH (14 ml), and water (10 ml). Purification via column chromatography (silica, cyclohexane:EtOAc; 1:1, $R_f = 0.513$) served 5H-chromeno

[4,3-b]bipyridin-5-ol **11** (475 mg, 2.38 mmol, 68%) as a yellow solid.

^1H NMR (800 MHz, $\text{DMSO}-d_6$, T = 293.15 K, δ): 8.67 (d, $^2J = 4.7$ Hz, $^3J = 1.6$ Hz, 1H), 8.23 (d, $^2J = 7.7$ Hz, $^3J = 1.7$ Hz, 1H), 7.81 (d, $^2J = 7.6$ Hz, $^3J = 1.7$ Hz, 1H), 7.59 (d, $^2J = 6.2$ Hz, 1H), 7.42–7.38 (m, 2H), 7.14 (t, $^2J = 7.5$ Hz, 1H), 7.07 (d, $^2J = 8.1$ Hz, $^3J = 1.3$ Hz, 1H), 6.46 (d, $^2J = 6.1$ Hz, 1H).

^{13}C NMR (200 MHz, $\text{DMSO}-d_6$, T = 293.15 K, δ): 152.8, 150.0, 146.1, 134.2, 131.1, 126.9, 123.9, 123.9, 123.0, 121.8, 121.5, 117.8, 92.07.

HR-MS (ESI⁺, EtOAc): $[\text{M} + \text{H}]^+$: $\text{C}_{12}\text{H}_9\text{NO}_2 + \text{H}^+$, calculated m/z 200.0706, found m/z 200.0707.

IR (KBr): $\nu = 2696.1, 1610.7, 1594.3, 1494.7, 1470.8, 1452.0, 1430.3, 1304.9, 1241.7, 1197.7, 1156.5, 1129.8, 1102.2, 1038.8, 990.8, 971.3, 883.1, 807.1, 791.6, 758.1, 722.4$ cm^{-1} .

2.4.8 | 8-(Trifluoromethyl)-5H-chromeno[4,3-b]pyridin-5-ol (**14**)

The reaction followed synthesis procedure **B**. 2-Chloronicotin-aldehyde (225 mg, 1.59 mmol), (2-hydroxy-4-(trifluoromethyl)-phenyl)boronic acid (491 mg, 2.38 mmol), sodium carbonate (656 mg, 6.2 mmol), and tetrakis (triphenylphosphine)-palladium (0) (184 mg, 159 μmol) were dissolved in DME (14 ml), EtOH (7 ml), and water (7 ml). Purification via column chromatography (silica, cyclohexane:EtOAc; 1:1, $R_f = 0.475$) served 8-(trifluoromethyl)-5H-chromeno[4,3-b]-bipyridin-5-ol **14** (260 mg, 973 μmol , 61%) as a light brown solid.

^1H NMR (600 MHz, CDCl_3 , T = 293.15 K, δ): 8.74 (d, $^2J = 4.8$ Hz, $^3J = 1.6$ Hz), 8.46 (d, $^2J = 8.1$ Hz, 1H, H8), 7.75 (d, $^2J = 7.7$ Hz, $^3J = 1.7$ Hz, 1H), 7.41 (d, $^2J = 8.1$ Hz, 1H), 7.38–7.35 (m, 2H), 6.56 (s, 1H).

^{13}C NMR (151 MHz, CDCl_3 , T = 293.15 K, δ): 152.2, 150.8, 145.5, 134.6, 126.2, 125.3, 124.5, 123.7, 122.7, 119.2, 115.27, 92.8.

MS (APCI⁺, 2-propanol): $[\text{M} + \text{H}]^+$: $\text{C}_{13}\text{H}_8\text{F}_3\text{NO}_2 + \text{H}^+$, calculated m/z 268.7, found m/z 268.1.

IR (KBr): $\nu = 3060.2, 1599.8, 1511.7, 1446.2, 1422.4, 1327.4, 1278.9, 1245.9, 1194.2, 158.0, 1138.0, 1125.8, 1109.3, 1052.8, 968.3, 948.1, 873.7, 837.7, 786.3, 724.5, 663.0$ cm^{-1} .

2.4.9 | 6H-Benzo[c]chromen-6-ol (**16**)

The reaction followed synthesis procedure **A**. 2-Bromophenol (1.00 g, 5.78 mmol), (2-formylphenyl)boronic acid (1.30 g, 8.67 mmol), sodium carbonate (1.41 g, 13.30 mmol), and bis (triphenylphosphine) palladium (II) dichloride (328 mg, 468 μmol) were

dissolved in THF (15 ml), MeOH (10 ml), and water (7 ml). Purification via column chromatography (silica, *n*-pentane:EtOAc; 4:1, $R_f = 0.740$) served 6*H*-naphtho[2,1-*c*]chromen-6-ol **16** (748 mg, 3.77 mmol, 65%) as a light brown solid.

NMR spectroscopic data were not assigned due to remaining impurities after purification with column chromatography. The identity of compound **16** was confirmed by HPLC-MS (cf. Figure 4).

IR (KBr): $\nu = 3085.2, 1608.3, 1487.2, 1457.9, 1439.6, 1296.8, 1242.2, 1194.5, 1126.7, 1098.0, 1055.2, 1029.7, 1015.5, 948.1, 811.7, 757.2, 717.9, 731.3 \text{ cm}^{-1}$.

HR-MS (ESI⁺, EtOAc): $[M-H_2O]^+$: C₁₃H₉O + H⁺, calculated m/z 181.0648, found m/z 181.0650.

2.4.10 | 3-Hydroxy-2-(4,4,5,5-tetramethyl-1,3,2-dioxaborolan-2-yl)benzaldehyde (**18**)

In a flame-dried Schlenk tube under argon, **17** (300 mg, 1.21 mmol, 1.00 equiv.), KOAc (356 mg, 3.63 mmol, 3.00 equiv.), B₂pin₂ (338 mg, 1.33 mmol, 1.10 equiv.), and Pd(dppf)₂Cl₂ (88.5 mg, 121 μ mol, 0.10 equiv.) were dissolved in DMF (5.6 ml) and stirred at 80°C. After 19 h, the solution was allowed to cool to RT., HCl (aqueous, 2 M, 10 ml) was added, and the solution was extracted with DCM (3 × 20 ml). The combined organic layers were washed with saturated aqueous Na/K-tartrate solution (10 ml) and dried over MgSO₄. Volatiles were removed in vacuo. The crude product was purified by column chromatography (silica, *n*-pentane/EtOAc 9:1 to 5:1) to give **18** (47.0 mg, 16%) as a brown solid.

¹H NMR (400 MHz, CDCl₃, T = 293.15 K, δ): δ 9.94 (s, 1H), 7.42 (s, 1H), 7.34 (s, 1H), 7.13 (m, 1H), 5.93 (s, 1H), 1.25 (s, 12H).

¹³C NMR (100 MHz, CDCl₃, T = 293.15 K, δ): 195.30, 164.89, 143.41, 133.40, 129.76, 121.74, 119.27, 85.13, 77.48, 24.96.

HR-MS (ESI⁺, CH₃CN): $[M + H]^+$: C₁₃H₁₈BO₄⁺, calculated m/z 249.1293, found m/z 249.1288.

IR (KBr): $\nu = 3364.9, 2996.3, 2974.8, 2929.9, 2876.8, 1689.0, 1618.8, 1592.8, 1493.5, 1479.6, 1443.4, 1380.6, 1370.2, 1304.0, 1278.2, 1233.0, 1000.0, 993.03, 960.8, 926.1, 944.6, 894.7, 875.0, 862.7, 803.9, 777.1, 745.5, 698.5, 680.7 \text{ cm}^{-1}$.

2.4.11 | 6,10-Dihydroxy-6*H*-benzo[*c*]chromene-1-carbaldehyde (**20**) 10-hydroxychromeno[5,4,3-*cde*]chromen-5(10*H*)-one (**21**)

In a flame-dried Schlenk tube under argon, **17** (23.0 mg, 121 μ mol, 1.00 equiv.), KOAc (66.9 mg, 484 mmol, 4.00

equiv.), **18** (30.0 mg, 121 μ mol, 1.00 equiv.), and Pd(dppf)₂Cl₂ (885 μ g, 1.21 μ mol, 0.01 equiv.) were dissolved in DMSO (1 ml). The reaction was stirred at 70°C for 24 h. After cooling to RT., EtOAc (10 ml) and water (10 ml) were added and the aqueous layer was extracted with EtOAc (2–20 ml). The combined organic layers were washed with a saturated aqueous solution of NaCl (5 ml) and dried over MgSO₄. Volatiles were removed in vacuo. The crude product was purified by flash column chromatography (silica, pentane:EtOAc; 5:1 to 3:1, $R_f = 0.312$) to give **20** and **21** (85.0 μ g, 0.3%) as a brown oil.

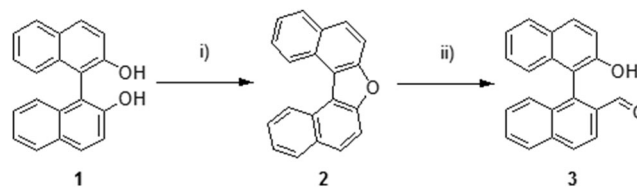
HR-MS (ESI⁺, EtOAc): **20** $[M + H]^+$: C₁₄H₁₁O₄⁺, calculated m/z 243.0652, found m/z 243.0646. **21** $[M + H]^+$: calculated m/z 241.0495, found m/z 241.049.

3 | RESULTS AND DISCUSSION

The sterically demanding binaphthyl hydroxy aldehyde **3** was prepared according to Martinez et al.,⁴⁴ to investigate the stereodynamics and the possibility to form the intramolecular hemiacetal. Starting from commercially available BINOL **1**, **3** could be obtained in 51% yield via a ring-closed intermediate product **2** by introducing an aldehyde function using dimethylformamide activated by lithium (cf. Scheme 1).

¹H-NMR analysis performed in deuterated chloroform (CDCl₃) showed that the binaphthyl structure **3** occurred exclusively in the open aldehyde form (cf. Figure 3), which can be explained by the steric hindrance of the naphthyl moieties, leading to the formation of atropisomers, which can be separated into their enantiomers by chiral HPLC using the CSP CHIRALPAK IC (*n*-hexane:isopropanol; 90:10) (cf. Figure 4).

Due to good availability and easy access to boronic acid derivatives and various halides, the biaryl hydroxy aldehyde derivatives **7**, **8**, **11**, **12**, **14**, and **16** were synthesized via Pd-catalyzed Suzuki C-C coupling reaction. After optimization of the reaction conditions, compounds **7** and **8** were obtained by Suzuki couplings between 1-Bromo-2-naphthaldehyde **6** and the corresponding commercially available boronic acids (cf. Scheme 2).



SCHEME 1 Synthesis route to **3** according to Martinez et al.⁴⁴ (i) *p*-TsOH, conc. HCl, toluene, 140°C, 5 days; (ii) Et₂O, toluene, Li, 0°C, 24 h → DMF, -78°C, 2 h → RT., 15 h.

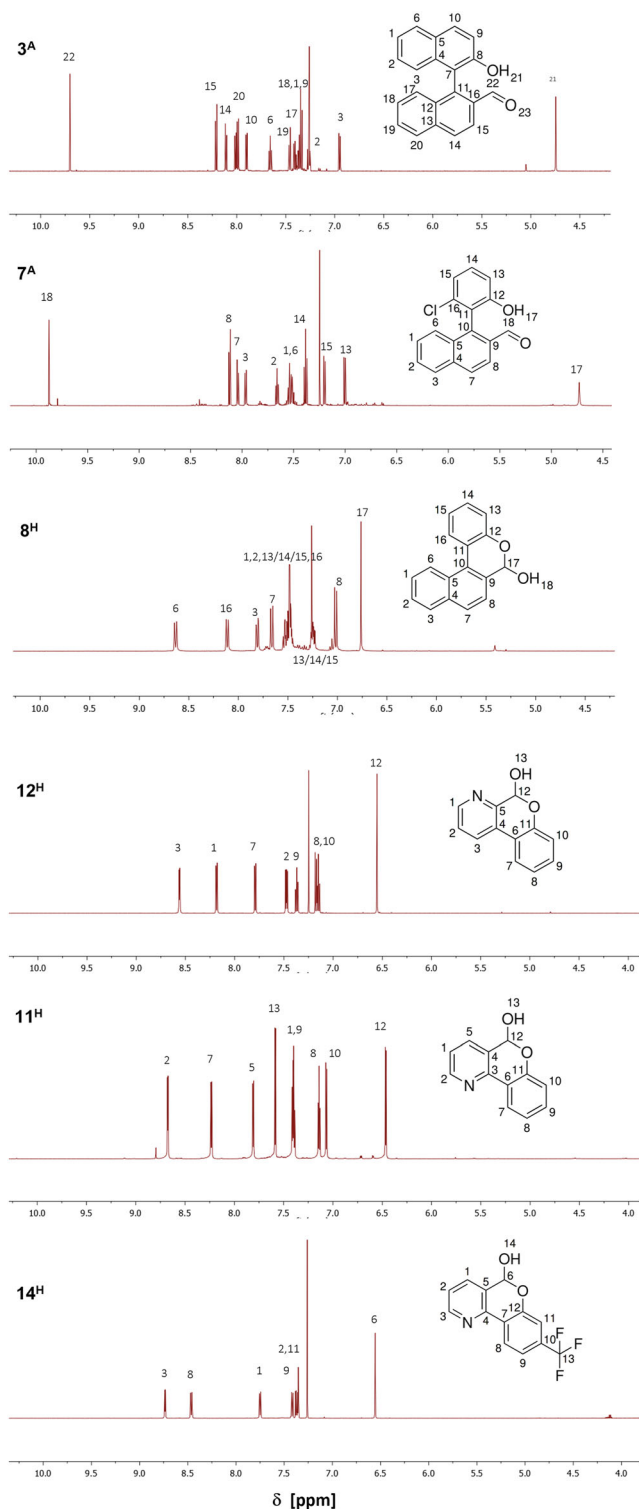


FIGURE 3 $^1\text{H-NMR}$ measurements in CDCl_3 at room temperature. X^{H} : Only the hemiacetal is present, X^{A} : Only the aldehyde is present.

Halogen aldehyde **6** was prepared from α -tetralone in a two-step synthesis.^{45,46}

The structural difference between the two structures **7** and **8** is the additional chlorine group in the 2-position

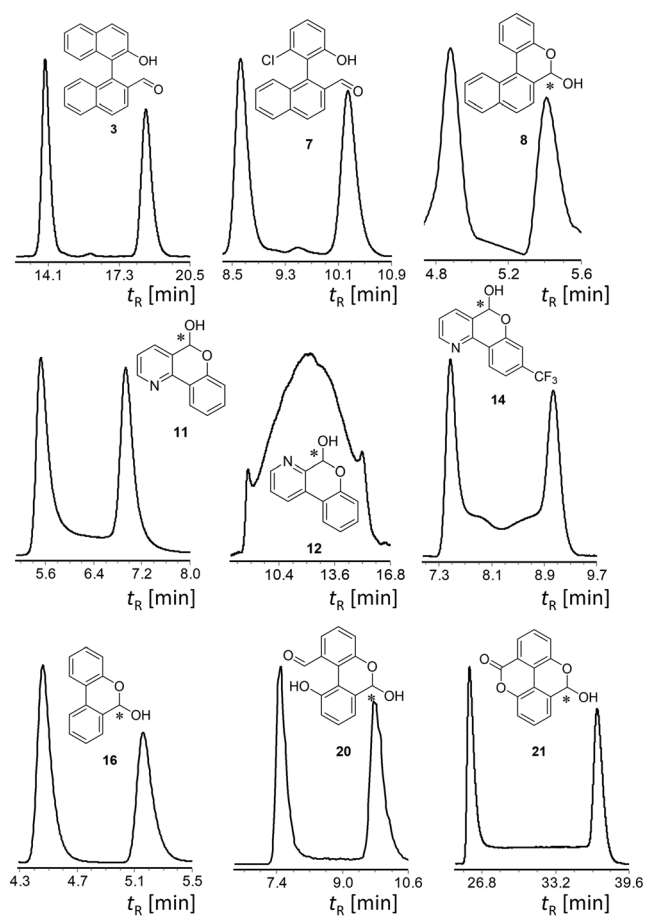
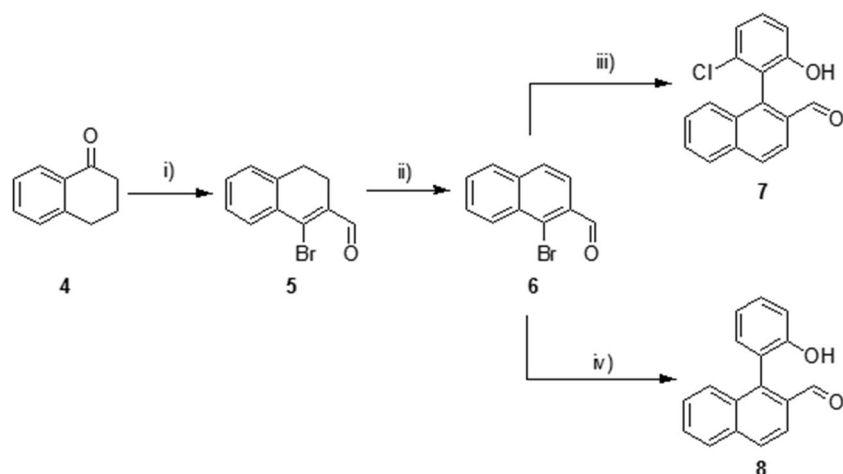
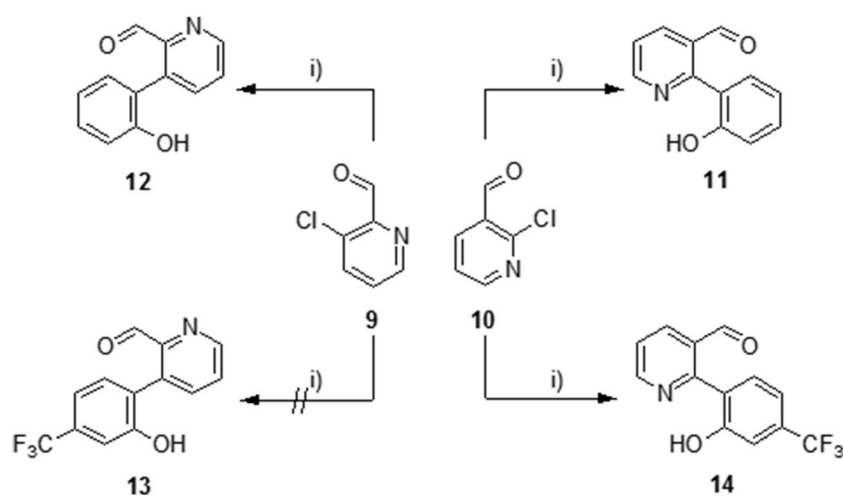


FIGURE 4 Chromatograms of the chiral HPLC separations at room temperature (except for compound **12**): **3** CHIRALPAK IC (*n*-hexane:isopropanol; 90:10), **7** and **8** CHIRALPAK IC (*n*-hexane:isopropanol; 80:20), **11** CHIRALPAK IA (*n*-hexane:isopropanol; 75:25), **12** CHIRALPAK IA (*n*-hexane:isopropanol; 80:20; 0°C), **14** CHIRALPAK IA (*n*-hexane:isopropanol; 95:5), **16** CHIRALPAK IA (*n*-hexane:isopropanol; 80:20), **20** and **21** CHIRALPAK IE (*n*-hexane:isopropanol; 85:15).

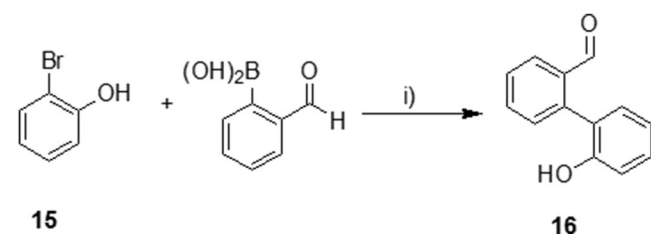
of the phenol moiety. Similar to binaphthyl derivative **3**, we observe for compound **7** only the ring-opened atropisomers, which is evident from the absence of the hemiacetal-signals in the $^1\text{H-NMR}$ spectrum (cf. Figure 3) and the separation of the atropisomers by chiral HPLC (cf. Figure 4). This agrees very well with the high stereointegrity observed for ortho-substituted chloro-biphenyl compounds.³⁵ In contrast to this, the nonsubstituted compound **8** exists only as intramolecularly ring-closed hemiacetal when dissolved in CDCl_3 (cf. Figure 3). To obtain the heterocyclic 2-phenylpyridine and 3-phenylpyridine hydroxy aldehydes **11–14**, commercially available chloro-pyridyl carbaldehydes **9** and **10** were coupled with corresponding boronic acids (Scheme 3). Surprisingly, 3-chloropicolin-aldehyde **9** could not be coupled with the trifluoromethyl substituted boronic acid to phenyl-pyridyl **13**.



SCHEME 2 Synthesis route to **7** and **8**. (i) PBr_3 , DMF, DCM, 0°C , 1 h $\rightarrow 90^\circ\text{C}$, 1 h⁴⁴; (ii) DMSO, Se, 180°C , 25 min; (iii) (2-chloro-6-hydroxyphenyl)boronic acid, Na_2CO_3 , Pd $(\text{PPh}_3)_4$, DME/ H_2O , 80°C reflux, 24 h; (iv) (2-hydroxyphenyl)boronic acid, Na_2CO_3 , Pd $(\text{PPh}_3)_2\text{Cl}_2$, THF/MeOH/ H_2O , 70°C reflux, 24 h.⁴⁶



SCHEME 3 Synthesis to **11**, **12**, and **14**. (i) Na_2CO_3 , (2-hydroxyphenyl)boronic acid, Pd $(\text{PPh}_3)_4$, DME, EtOH, 80°C , 24 h.



SCHEME 4 Synthesis of **16**. (i) Na_2CO_3 , (2-formylphenyl)boronic acid, Pd $(\text{PPh}_3)_2\text{Cl}_2$, THF, MeOH, 70°C , 24 h.

All obtained 2-phenylpyridines **11** and **14**, and the 3-phenylpyridine **12** formed the corresponding hemiacetal according to $^1\text{H-NMR}$ analysis in CDCl_3 . The less sterically demanding phenylpyridines and the electron-deficient heterocycle seem to favor and stabilize the hemiacetal form.

The core structure of the biaryl aldehyde-alcohols **16**, which was obtained in a Suzuki reaction of 2-bromophenol and (2-formylphenyl)boronic acid (cf. Scheme 4), was expected to favor the ring closure to form an intramolecular hemiacetal. In comparison, we

have observed the hemiacetal formation already in structure **8** (vide supra), whereas with the binaphthyl system, **3** no hemiacetals are formed. Indeed, the $^1\text{H-NMR}$ spectrum in CDCl_3 shows mainly the presence of the hemiacetal structure (cf. Figure 3). Although a second species, which is the corresponding lactone, formed by autooxidation, was identified by MS analysis. Due to this unavoidable side reaction, unambiguous assignment of the NMR signals is not possible.

In the next step, we considered the synthesis of double functionalized biaryl aldehyde-alcohols to study the formation and properties of double ring-closed structures.

Compound **17** was synthesized following Botelho et al.⁴⁷ A boronic acid pinacol ester was introduced obtaining **18**,⁴⁸ which was then coupled with **17** in a Suzuki Miyaura reaction to obtain **19**²⁴ (cf. Scheme 5). However, **19** could not be isolated, due to its very sensitive nature and the fact that it exists only in equilibrium with the mono-hemiacetal **20** and reacts to the partially oxidized hemiacetal-lactone **21**, identified by HPLC

SCHEME 5 Synthesis of compounds **19**, **20**, and **21**. (i) B_2pin_2 , KOAc, Pd (dppf) $_2Cl_2$, DMSO, 80°C, 23 h, (ii) K_2CO_3 , **17**, Pd (dppf) $_2Cl_2$, DMSO, 70°C, 24 h.

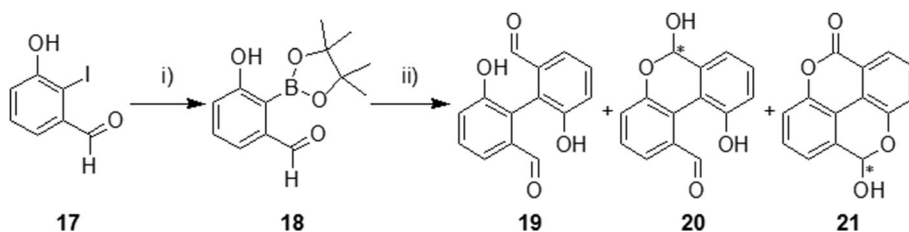


TABLE 1 Summarized results of the solvent dependent NMR measurements.

Solvent/substance	3	7	8	11	12	14	16
Acetone- d_6	A	A	H	H	H	H	H
DMSO- d_6	A	A	H	H	H	H	H
THF- d_8	A	A	H	H	H	H	H
DCM- d_2	A	A	H	H	H	H	H
Toluene- d_8	A	A	H	H	H	H	H

Note: Substance only present in aldehyde form (A) or hemiacetal form (H).

measurements. Consequently, while investigating these compounds by chiral HPLC, not only the hemiacetal interconversion of **20** but also the interconversion of the hemiacetal-lactone **21** could be observed in a single chromatographic run.

3.1 | Solvent dependent NMR experiments

All NMR measurements performed in $CDCl_3$ gave exclusively hints to the favored formation of the hemiacetal (H) or the opened form as aldehyde-alcohol (A) **3^A**, **7^A**, **8^H**, **11^H**, **12^H**, **14^H**, and **16^H** (cf. Figure 3). Because ring closure and opening can be highly solvent dependent, for example, because of acidity or solubility, we screened compounds **3**, **4**, **7**, **8**, **11**, **14**, and **16** in five deuterated solvents (Table 1). Characteristic NMR signals of the aldehyde^A or the hemiacetal^H were used to determine potential ratios between open and closed form. The NMR measurements were performed after dissolving the compounds and repeated twice at intervals of several days. Surprisingly, these compounds were very stable in their favored form and independent of the solvent.

3.2 | Enantioselective dynamic HPLC (DHPLC) analysis

All the investigated structures here are chiral. In the ring-opened form, these compounds exist as *tropos* isomers or atropisomers and upon intramolecular ring

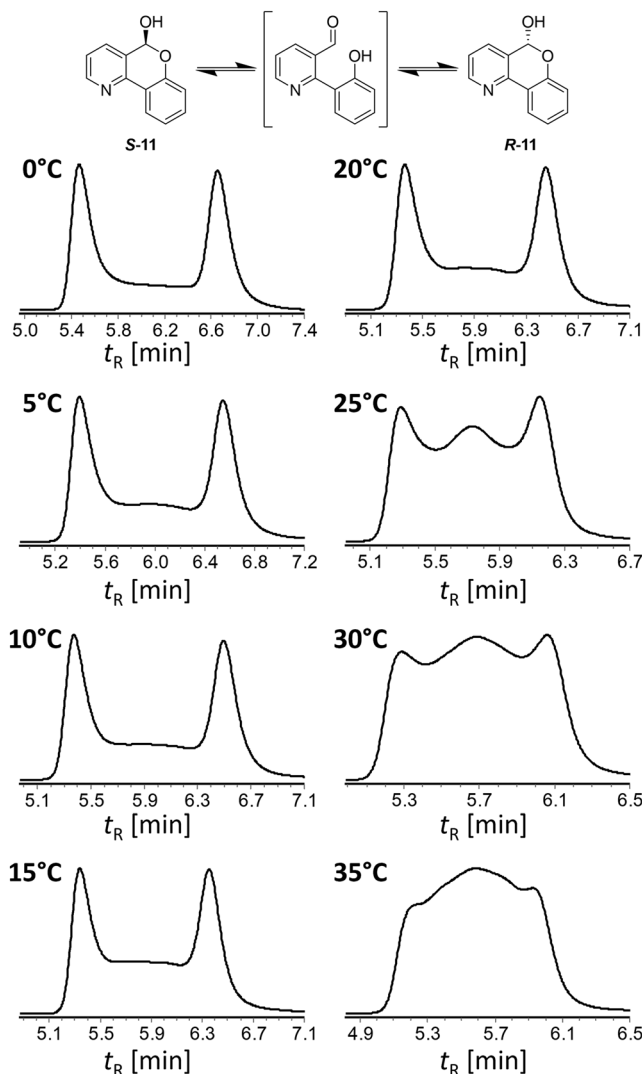


FIGURE 5 Selected chromatograms obtained by enantioselective DHPLC of **11** at temperatures between 0 and 35°C. CHIRALPAK IA (*n*-hexane:isopropanol; 90:10).

closure as hemiacetals. The hemiacetals form enantiomers or in case of the double aldehyde-alcohols enantiomers and the meso isomer. The opened aldehydes **3^A** and **7^A** are axially chiral and can be separated into the enantiomers by chiral HPLC.

The separation of the hemiacetals **8^H**, **11^H**, **12^H**, **14^H**, **16^H**, **20^H**, and **21^H** into the enantiomers was achieved by HPLC using immobilized chiral stationary polysaccharide

phases⁴⁹ and identified by MS detection (cf. Figure 4). The 2-phenylpyridine derivatives, compounds **11^H** and **14^H** as well as compounds **20^H** and **21^H**, showed significant (**11^H** and **14^H**) and slight (**20^H** and **21^H**) plateau

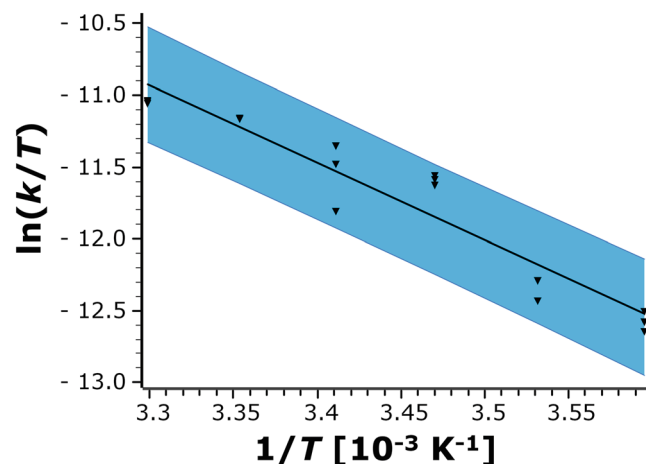


FIGURE 6 Eyring-plot of compound **11** obtained by enantioselective DHPLC to determine the activation parameters of enantiomerization. The error band represents the level of confidence of 95% of the linear regression. For the linear regression, three measurements at each temperature were considered.

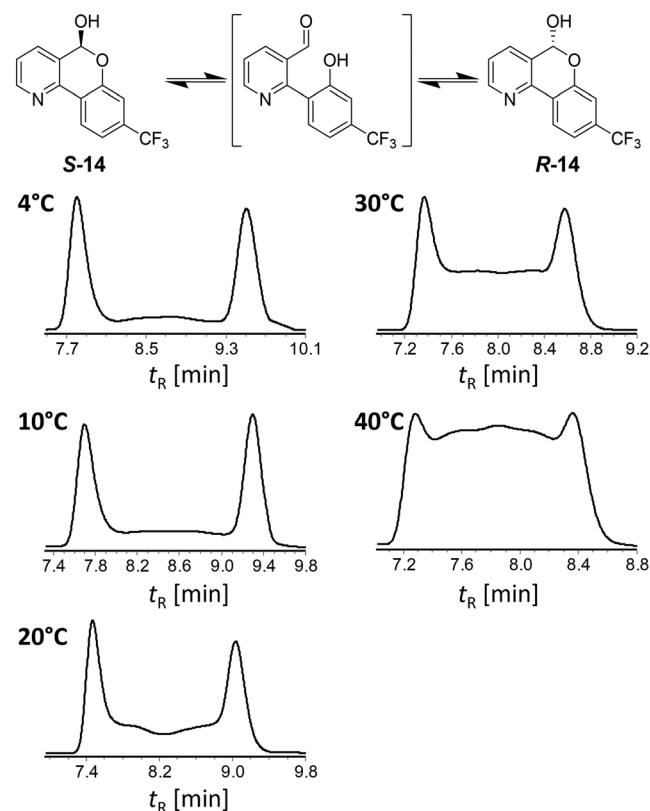


FIGURE 7 Selected chromatograms obtained by enantioselective DHPLC of **14** at temperatures between 4 and 40 °C. Chiralpak IA (*n*-hexane:isopropanol; 90:10).

formation at room temperature due to the interconversion of the hemiacetal enantiomers (cf. Figure 4). Therefore, we performed temperature dependent enantioselective DHPLC measurements to determine the

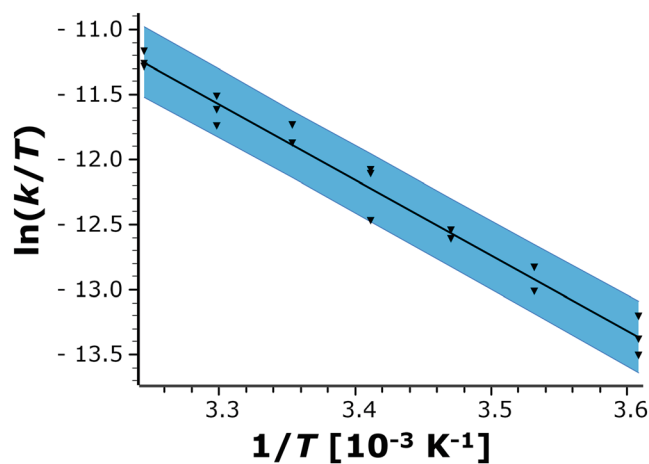


FIGURE 8 Eyring-plot of compound **14** obtained by enantioselective DHPLC to determine the activation parameters of enantiomerization. The error band represents the level of confidence of 95% of the linear regression. For the linear regression, three measurements at each temperature were considered.

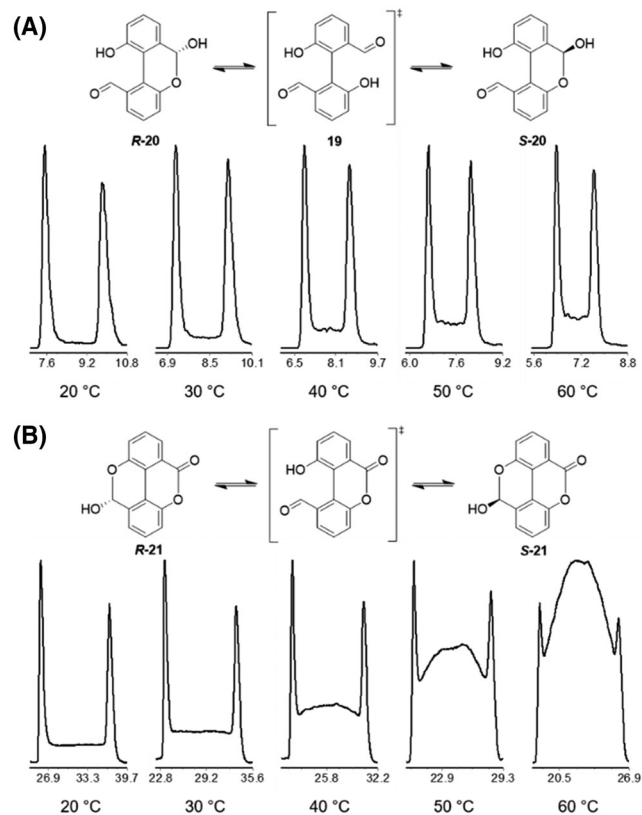


FIGURE 9 Selected chromatograms obtained by enantioselective DHPLC of (A) **20**, and (B) **21** at temperatures between 4 and 40 °C. Chiralpak IE (*n*-hexane:isopropanol; 85:15).

enantiomerization barriers ΔG^\ddagger and the activation parameters ΔH^\ddagger and ΔS^\ddagger by Eyring-plot analysis. The enantiomerization rate constants k_1 were determined by analysis of the chromatographic peak profiles using the unified equation of dynamic chromatography⁵⁰ implemented in the software DCXplorer.⁵¹ For the two 2-phenylpyridine derivatives **11^H** (Figures 5 and 6), we determined the activation barrier to be $\Delta G^\ddagger = 86.4 \text{ kJ}\cdot\text{mol}^{-1}$ and the activation parameters $\Delta H^\ddagger = 47.2 \pm 3 \text{ kJ}\cdot\text{mol}^{-1}$ and $\Delta S^\ddagger = -132 \pm 22 \text{ J}\cdot(\text{K}\cdot\text{mol})^{-1}$ between 0 and 35°C, and for **14^H** (Figures 7 and 8) $\Delta G^\ddagger = 85.0 \text{ kJ}\cdot\text{mol}^{-1}$, $\Delta H^\ddagger = 33.2 \pm 3 \text{ kJ}\cdot\text{mol}^{-1}$ and $\Delta S^\ddagger = -174 \pm 96 \text{ J}\cdot(\text{K}\cdot\text{mol})^{-1}$ between 4 and 40°C.

The most pronounced plateau formation caused by rapid enantiomerization was observed for compound **12^H** already at a temperature as low as 0°C. The enantiomerization rate constant was determined to be $k_1 = 4.9 \cdot 10^{-3} \text{ s}^{-1}$ and the enantiomerization barrier

$\Delta G^\ddagger = 78.8 \text{ kJ}\cdot\text{mol}^{-1}$. Measurements at elevated temperatures led to complete peak coalescence.⁵² This represents a significant decrease of $4.3 \text{ kJ}\cdot\text{mol}^{-1}$ compared to the enantiomerization barrier of compound **11^H** at 0°C. Structurally, the difference is due to the position of the N atom in the pyridine ring. In ortho-position, a destabilization of the hemiacetal is observable.

For compounds **20^H** and **21^H**, the enantiomerization barriers ΔG^\ddagger and the activation parameters ΔH^\ddagger and ΔS^\ddagger were determined by enantioselective DHPLC measurements. For lactone **21^H**, we obtained the following parameters: $\Delta G^\ddagger = 89.8 \text{ kJ}\cdot\text{mol}^{-1}$, $\Delta H^\ddagger = 35.3 \pm 0.6 \text{ kJ}\cdot\text{mol}^{-1}$, and $\Delta S^\ddagger = -183 \pm 38 \text{ J}\cdot(\text{K}\cdot\text{mol})^{-1}$. The enantiomerization barrier is slightly higher for hemiacetal **20^H**: $\Delta G^\ddagger = 91.2 \text{ kJ}\cdot\text{mol}^{-1}$, $\Delta H^\ddagger = 27.8 \pm 1.2 \text{ kJ}\cdot\text{mol}^{-1}$, and $\Delta S^\ddagger = -213 \pm 40 \text{ J}\cdot(\text{K}\cdot\text{mol})^{-1}$ (cf. Figures 9 and 10). These two compounds were measured simultaneously from the same sample, which demonstrates the advantage of DHPLC not requiring a purification of the samples and isolation of the single compounds.

All other separated enantiomers were also screened in temperature-dependent experiments; however, no plateau formation could be observed in measurements of up to 80°C.

4 | CONCLUSION

Here, we presented easily accessible synthetic routes via largely commercially available starting materials to biaryl aldehyde-alcohols forming hemiacetals by intramolecular ring closure (**8**, **11**, **12**, **14**, **16**, **20**, and **21**), which can be considered as homologs of coumarin. Compounds **3**³² and **7** form atropisomers and are unable to undergo ring closure because of steric hindrance. The enantiomerization of these atropisomers was not observed, even for temperatures of up to 60°C. The biaryl aldehyde-alcohols **8**, **11**, **12**, **14**, **16**, **20**, and **21** prefer the hemiacetal form. For compounds **11**, **14**, **20**, and **21**, the enantiomerization barriers of the hemiacetal interconversion were determined by temperature dependent enantioselective DHPLC experiments. The interconversion barriers are in excellent agreement with the interconversion barriers and barriers of formation of the transient hemiacetal catalysts formed in Soai's asymmetric autocatalysis.²³

ACKNOWLEDGMENTS

Generous financial support by the European Research Council (ERC) for a Starting Grant (No. 258740, AMP-CAT) is acknowledged. Open Access funding enabled and organized by Projekt DEAL.

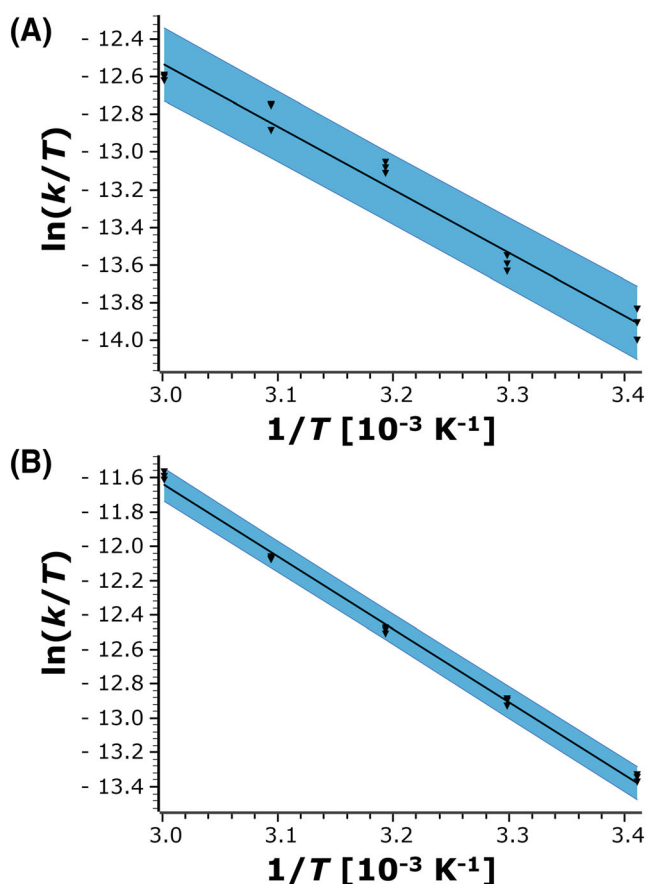


FIGURE 10 Eyring-plot of compounds (A) **20** and (B) **21** obtained by enantioselective DHPLC to determine the activation parameters of enantiomerization. The error band represents the level of confidence of 95% of the linear regression. For the linear regression, three measurements at each temperature were considered.

DATA AVAILABILITY STATEMENT

All data are included in the manuscript. Chromatographic and spectroscopic raw data are available from the corresponding author upon request.

ORCID

Yanis Luca Pignot  <https://orcid.org/0000-0003-1087-285X>

Oliver Trapp  <https://orcid.org/0000-0002-3594-5181>

REFERENCES

- Blackmond DG. Autocatalytic models for the origin of biological homochirality. *Chem Rev.* 2020;120:4831-4847.
- Huber L, Trapp O. Symmetry breaking by consecutive amplification: efficient paths to homochirality. *Orig Life Evol Biosph.* 2022;52:75-91.
- Geiger Y, Achard T, Maise-François A, Bellemin-Laponnaz S. Hyperpositive nonlinear effects in asymmetric catalysis. *Nature Catalysis.* 2020;3:422-426.
- Geiger Y, Achard T, Maise-François A, Bellemin-Laponnaz S. Observation of hyperpositive non-linear effect in catalytic asymmetric organozinc additions to aldehydes. *Chirality.* 2020; 32:1250-1256.
- Buhse T, Cruz J-M, Noble-Terán ME, et al. Spontaneous deracemizations. *Chem Rev.* 2021;121:2147-2229.
- Soai K. The Soai reaction and its implications with the life's characteristic features of self-replication and homochirality. *Tetrahedron.* 2022;124:133017.
- Soai, K, Niwa S, Hori H, Asymmetric self-catalytic reaction. Self-production of chiral 1-(3-pyridyl)alkanols as chiral self-catalysts in the enantioselective addition of dialkylzinc reagents to pyridine-3-carbaldehyde. *J Chem Soc Chem Commun* 1990; 982-983, 14, doi:10.1039/c39900000982.
- Soai K, Shibata T, Morioka H, Choji K. Asymmetric autocatalysis and amplification of enantiomeric excess of a chiral molecule. *Nature.* 1995;378:767-768.
- Sato I, Omiya D, Igarashi H, et al. Relationship between the time, yield, and enantiomeric excess of asymmetric autocatalysis of chiral 2-alkynyl-5-pyrimidyl alkanol with amplification of enantiomeric excess. *Tetrahedron: Asymmetry.* 2003;14:975-979.
- Matsumoto A, Tanaka A, Kaimori Y, Hara N, Mikata Y, Soai K. Circular dichroism spectroscopy of catalyst preequilibrium in asymmetric autocatalysis of pyrimidyl alkanol. *Chem Commun.* 2021;57:11209-11212.
- Matsumoto A, Abe T, Hara A, et al. Crystal structure of the isopropylzinc alkoxide of pyrimidyl alkanol: mechanistic insights for asymmetric autocatalysis with amplification of enantiomeric excess. *Angew Chem Int Ed.* 2015;54:15218-15221.
- Blackmond DG. Mechanistic study of the Soai autocatalytic reaction informed by kinetic analysis. *Tetrahedron: Asymmetry.* 2006;17:584-589.
- Gridnev ID, Serafimov JM, Quiney H, Brown JM. Reflections on spontaneous asymmetric synthesis by amplifying autocatalysis. *Org Biomol Chem.* 2003;1:3811-3819.
- Gehring T, Quaranta M, Odell B, Blackmond DG, Brown JM. Observation of a transient intermediate in Soai' asymmetric autocatalysis: insights from ¹H NMR turnover in real time. *Angew Chem Int Ed.* 2012;51:9539-9542.
- Romagnoli C, Sieng B, Amedjkouh M. Kinetic relationship in parallel autocatalytic amplifications of pyridyl alkanol and chiral trigger pyrimidyl alkanol. *Chirality.* 2020;32:1143-1151.
- Funes-Maldonado M, Sieng B, Amedjkouh M. Asymmetric autocatalysis as a relay for remote amplification of chirality of target molecules used as triggers. *Org Lett.* 2016;18: 2536-2539.
- Rotunno G, Petersen D, Amedjkouh M. Absolute autocatalytic amplification under heterogenous phase conditions involving subsequent hydride transfer and a hemiacetal intermediate. *ChemSystemsChem.* 2020;2:e1900060.
- Podlech J, Gehring T. New aspects of Soai's asymmetric autocatalysis. *Angew Chem Int Ed.* 2005;44:5776-5777.
- Athavale SV, Simon A, Houk KN, Denmark SE. Structural contributions to autocatalysis and asymmetric amplification in the Soai reaction. *J Am Chem Soc.* 2020;142:18387-18406.
- Athavale SV, Simon A, Houk KN, Denmark SE. Demystifying the asymmetry-amplifying, autocatalytic behaviour of the Soai reaction through structural, mechanistic and computational studies. *Nat Chem.* 2020;12:412-423.
- Trapp O, Lamour S, Maier F, Siegele AF, Zawatzky K, Straub BF. In situ mass spectrometric and kinetic investigations of Soai's asymmetric autocatalysis. *Chem a Eur J.* 2020;26: 15871-15880.
- Trapp O. Efficient amplification in Soai's asymmetric autocatalysis by a transient stereodynamic catalyst. *Front Chem.* 2020;8: 1173.
- Geiger Y. One Soai reaction, two mechanisms? *Chem Soc Rev.* 2022;51:1206-1211.
- Mahlau M, List B. Asymmetric Counteranion-directed catalysis: concept, definition, and application. *Angew Chem Int Ed.* 2013;52:518-533, 2. doi:10.1002/anie.201205343
- Jung M, Fluck M, Schurig V. Enantiomerization of 2,2'-diisopropylbiphenyl during chiral inclusion gas chromatography: determination of the rotational energy barrier by computer simulation of dynamic elution profiles. *Chirality.* 1994;6:510-512.
- Maier F, Trapp O. Effects of the stationary phase and the solvent on the stereodynamics of BIPHEP ligands quantified by dynamic three-column HPLC. *Angew Chem Int Ed.* 2012;51: 2985-2988.
- Wolf C, König WA, Roussel C. Influence of substituents on the rotational energy barrier of atropisomeric biphenyls - studies by polarimetry and dynamic gas chromatography. *Liebigs Ann.* 1995;781-786.
- Wolf C, König WA, Roussel C. Conversion of a racemate into a single enantiomer in one step by chiral liquid chromatography: studies with rac-2,2'-diiodobiphenyl. *Chirality.* 1995;7(8):610-611. doi:10.1002/chir.530070809
- Weseloh G, Wolf C, König WA. A new application of capillary zone electrophoresis: determination of energy barriers of configurationally labile chiral compounds. *Angew Chem Int Ed.* 1995; 34(15):1635-1636. doi:10.1002/anie.199516351
- Biedermann PU, Schurig V, Agranat I. Enantiomerization of environmentally significant overcrowded polychlorinated biphenyls (pcbs). *Chirality.* 1997;9(4):350-353. doi:10.1002/(SICI)1520-636X(1997)9:4<350::AID-CHIR6>3.0.CO;2-H

31. Auras S, Trapp O. Diastereoselective synthesis of a cyclic diamide-bridged biphenyl as chiral atropos ligand. *Chirality*. 2022;34:813-819.
32. Mislow K, Bolstad R. Molecular dissymmetry and optical inactivity. *J Am Chem Soc*. 1955;77:6712-6713.
33. Mezey PG. Mislow's label paradox, chirality-preserving conformational changes, and related chirality measures. *Chirality*. 1998;10:173-179.
34. Mikami K, Matsukawa S. Asymmetric synthesis by enantiomer-selective activation of racemic catalysts. *Nature*. 1997;385:613-615.
35. Mayer LC, Heitsch S, Trapp O. Nonlinear effects in asymmetric catalysis by design: concept, synthesis, and applications. *Acc Chem Res*. 2022;55:3345-3361.
36. Aikawa K, Mikami K. Asymmetric catalysis based on tropes ligands. *Chem Commun*. 2012;48(90):11050-11069. doi:10.1039/c2cc34320g
37. Diéguez M, Pàmies O, Moberg C. Self-adaptable tropes catalysts. *Acc Chem Res*. 2021;54(16):3252-3263. doi:10.1021/acs.accounts.1c00326
38. Bringmann G, Breuning M, Endress H, Vitt D. Biaryl Hydroxy aldehydes as intermediates in the metal-assisted atropo-enantioselective reduction of biaryl lactones: structures and aldehyde-lactol equilibria. *Tetrahedron*. 1998;54:10677-10690.
39. Veciana J, Crespo MI. Dynamic HPLC, a method for the determination of rate constants, energy barriers and equilibrium constants of dynamic molecular processes. *Angew Chem Int Ed*. 1991;30:74-77.
40. Trapp O. Interconversion of stereochemically labile enantiomers (enantiomerization). *Top Curr Chem*. 2013;341:231-270.
41. Trapp O, Schoetz G, Schurig V. Determination of enantiomerization barriers by dynamic and stopped flow chromatographic methods. *Chirality*. 2001;13(8):403-414. doi:10.1002/chir.1052
42. D'Acquarica I, Gasparrini F, Pierini M, Villani C, Zappia G. Dynamic hplc on chiral stationary phases: a powerful tool for the investigation of stereomutation processes. *J Sep Sci*. 2006;29:1508-1516.
43. Wolf C. *Dynamic stereochemistry of chiral compounds - principles and applications*. Cambridge: RSC Publishing; 2008.
44. Yang J, Chatelet B, Dufaud V, et al. Enantio- and substrate-selective recognition of chiral neurotransmitters with C3-symmetric switchable receptors. *Org Lett*. 2020;22:891-895.
45. Moleele SS, Michael JP, de Koning CB. Tetralones as precursors for the synthesis of 2,20 -disubstituted 1, 10 -binaphthyls and related compounds. *Tetrahedron*. 2006;62:2831-2844.
46. Mikhaylov AA, Dilman AD, Novikov RA, et al. Tandem Pd-catalyzed C-C coupling/recyclization of 2(2-bromoaryl) cyclopropane-1,1-dicarboxylates with primary nitroalkanes. *Tetrahedron Lett*. 2016;57:11-14.
47. Serra A, Pineiro M, Santos AM, Rocha Gonsalves AMda, Abrantes M, Laranjo M, Botelho MF, in vitro photodynamic activity of 5,15-bis(3-Hydroxyphenyl)porphyrin and its halogenated derivatives against cancer cells. *Photochem Photobiol*. 2010;86:206-212.
48. Skaff O, Jolliffe KA, Hutton CA. Synthesis of the side chain cross-linked tyrosine oligomers Dityrosine, Trityrosine and Pulcherosine. *J Org Chem*. 2005;70:7353-7363.
49. Ikai T, Okamoto Y. Structure control of polysaccharide derivatives for efficient separation of enantiomers by chromatography. *Chem Rev*. 2009;109:6077-6101.
50. Trapp O. Unified equation for access to rate constants of first-order reactions in dynamic and on-column reaction chromatography. *Anal Chem*. 2006;78:189-198.
51. Trapp O. A novel software tool for high throughput measurements of interconversion barriers: DCXplorer. *J Chromatogr B*. 2008;875:42-47.
52. Schurig V. Peak coalescence phenomena in enantioselective chromatography. *Chirality*. 1998;10:140-146.

How to cite this article: Heitsch S, Mayer LC, Pignot YL, Trapp O. Synthesis and stereodynamics of intramolecular hemiacetals in biaryl aldehyde-alcohols. *Chirality*. 2023;35(9):549-561. doi:10.1002/chir.23560